Proceedings of ICRC 2001: 745 © Copernicus Gesellschaft 2001

ICRC 2001

Atmospheric monitoring for the Auger Fluorescence Detector

J. A. J. Matthews[1], **Roger Clay**[2], **for the the Pierre Auger Observatory Collaboration**[3]

[1]University of New Mexico, Albuquerque, NM 87131
[2]University of Adelaide, Adelaide, Australia 5005
[3]Observatorio Pierre Auger, Av. San Martin Norte 304, (5613) Malargüe, Argentina

Abstract. A subset of all of the showers observed by the Auger experiment will be measured by both the ground array and the fluorescence detectors. These special *hybrid* events will be used to set the shower energy scale (based on the fluorescence detector determination of the shower energies) and to measure the shower energy resolution for the experiment. The largest uncertainties in the fluorescence measurement come from uncertainties in the atmospheric transmission, air Cherenkov subtraction, light multiple-scattering and cloud corrections to the fluorescence data. The Auger program of atmospheric monitoring, formulated to minimize these uncertainties, is summarized.

1 Air Shower Measurements by Fluorescence Detectors

Extreme high energy (EHE) cosmic rays produce extensive air showers in the atmosphere. Approximately 50 parts per million of the deposited energy is isotropically re-radiated in fluorescence emission at near-UV wavelengths: $290 \sim 440$nm. Fluorescence detectors measure the cascade by observing the shower grow in brightness, reach maximum and then decrease in brightness. The integral of the longitudinal development profile reveals the total electromagnetic shower energy.

Atmospheric corrections to Auger fluorescence data can be understood by noting that the atmosphere, in addition to being the showering medium for the primary cosmic ray, is an essential part of the readout system. Thus, like any component of a readout system, the atmosphere must be calibrated, the calibration monitored with time and the atmospheric calibrations input to the analysis of the fluorescence data. To minimize the atmospheric uncertainties, fluorescence experiments are located in dry desert areas with typically excellent visibility.

The Auger energy measurements will depend on the precision of the air fluorescence measurements which, in turn, depend on several uncertainties. Two of these, the fraction of detectable shower energy (Song et al., 1999) and the fraction of electromagnetic energy loss (in air) that appears as fluorescence light (Kakimoto et al., 1996), contribute $\sim 5\%$ and $\sim 10\%$ systematic uncertainties respectively to the fluorescence energy measurement. The other major uncertainties come from the calibration of the absolute efficiency of the fluorescence telescopes and from the precision of various atmospheric transmission, air Cherenkov subtraction, light multiple-scattering and cloud corrections to the fluorescence data. The Auger program of atmospheric monitoring, formulated to minimize these uncertainties, is summarized below.

Correspondence to: J. A.J. Matthews
(johnm@dot.phys.unm.edu)

2 Atmospheric Characterization and Corrections in Auger

The observed light intensity after scattering, I, can be related to the light intensity of the (isotropic) fluorescence source, I_0, as follows:

$$I \;=\; I_0 \cdot T^m \cdot T^a \cdot (1. \;+\; H.O.) \cdot \frac{d\Omega}{4\pi}$$

where T^m and T^a are the transmission factors for the *molecular* and *aerosol* scattering, $H.O.$ is a higher order correction (also known as multiple-scattering or aureole) and $d\Omega$ is the solid angle subtended by the observing telescope. Uncertainties in the source light intensity will arise from uncertainties in each of the (correction) factors in the expression. As the shower energy is proportional to the fluorescence light signal, the relative uncertainty in the reconstructed shower energy, E, is the same as the combined relative uncertainty in the transmission.

Rayleigh scattering describes the scattering of light in a pure or molecular atmosphere, and Mie scattering describes the scattering of light on much larger scattering centers in the atmosphere called aerosols. In practice the Rayleigh scattering related corrections, while large, can be made with precision using conventional atmospheric data: the temperature and pressure at the fluorescence detectors, and the adiabatic model for the atmosphere (Martin et al., 1999). In contrast the corrections related to Mie scattering, while typically less than the Rayleigh corrections, are *a priori* unknown. Thus

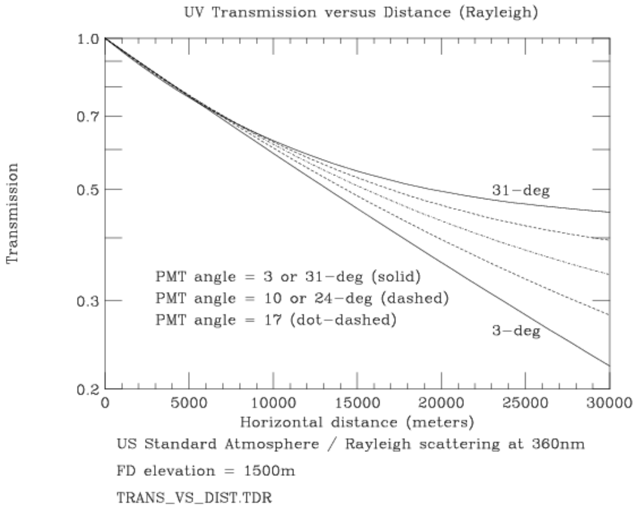

Fig. 1. Transmission factor, T^m, for Rayleigh scattering on the molecular atmosphere. Curves are shown for Auger fluorescence telescope viewing angles from $3^\circ \sim 31^\circ$ to the horizon.

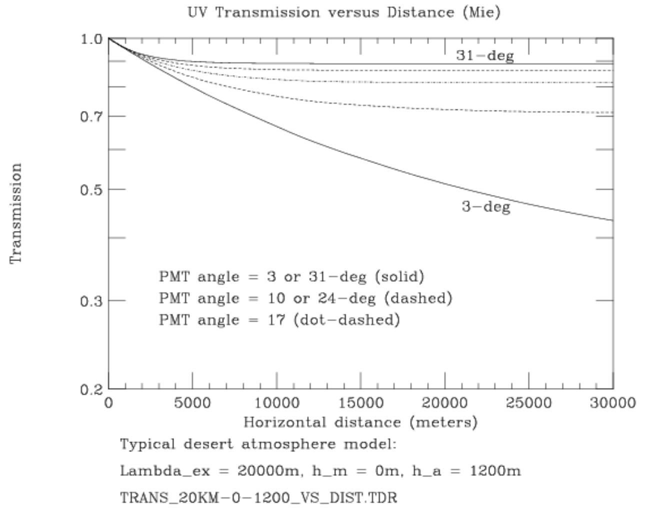

Fig. 2. Transmission factor, T^a, for Mie scattering on aerosols in the atmosphere. The aerosols are described by a horizontal extinction length, $\Lambda^a(360nm) = 20$km and an exponential scale height, $h_a = 1200$m. Curves are shown for Auger fluorescence telescope viewing angles from $3^\circ \sim 31^\circ$ to the horizon.

most of the atmospheric monitoring is focused on the aerosol (Mie scattering) component.

The transmission corrections depend on the Rayleigh and Mie total scattering cross sections and on the integral of the scatterer densities. This is summarized in Sect. 2.1 below. The air Cherenkov (Cassiday et al., 1990) and multiple scattering ($H.O.$) corrections depend on the differential scattering cross sections and on the local density of scatterers. The measurement and monitoring of the Mie aerosol phase function (normalized differential scattering cross section) is summarized in Sect. 2.2 below.

2.1 Transmission Correction

It is instructive to review the form of the Rayleigh transmission factor (which causes the apparent intensity from a source to decrease exponentially with travel distance through the atmosphere). The multiplicative *molecular transmission* is given by:

$$T^m \equiv T^m(z,\alpha,\lambda) = e^{-\int_0^z \frac{\rho^m(z)dz}{\Lambda^m(\lambda)} \cdot \frac{1}{sin(\alpha)}}$$

where z is the vertical height of the light source above the fluorescence telescope. $\rho^m(z)$ is the air density and α is the elevation angle of the light path. Finally $\Lambda^m(\lambda) = 2974 \cdot (\frac{\lambda}{400nm})^4$ gm/cm^2 is the Rayleigh extinction length (Flowers et al., 1969). At an Auger site altitude of ~ 1500m, this corresponds to $\Lambda^m(\lambda) \sim 18.4$ km at 360nm (approximate middle of Auger fluorescence detector wavelength acceptance).

The molecular transmission, T^m, factors into a height-wavelength dependent *molecular optical depth*:

$$\tau^m(z,\lambda) = \int_0^z \frac{\rho(z)dz}{\Lambda^m(\lambda)}$$

and into a slant factor, $\frac{1}{sin(\alpha)}$, where $\frac{z}{sin(\alpha)}$ is the full length of the light path. This factorization reflects the 1-dimensional nature of the molecular atmosphere. The further factorization of $\tau^m(z,\lambda)$ into a height dependent part, $\int_0^z \rho(z)dz$, and into a wavelength dependent part, $\frac{1}{\Lambda^m(\lambda)}$, reflects the fact that the composition of the molecular atmosphere is independent of height.

The 1-dimensional Rayleigh atmosphere provides a guide to model the multiplicative (Mie) *aerosol transmission* where we now use $\tilde{\rho}^a(z) = \rho^a(z)/\rho^a(0)$ as the normalized density of aerosols *versus* altitude. It is typical, but not essential, to parameterize $\tilde{\rho}^a(z)$ as $\tilde{\rho}^a(z) = e^{-z/h_a}$; h_a is the aerosol (vertical) scale height. $\Lambda^a(\lambda)$ is the aerosol extinction length as a function of wavelength measured at the height of the fluorescence telescopes.

Representative examples of molecular (Rayleigh) and aerosol (Mie) transmission factors are shown in Fig. 1 and 2 respectively. The transmission factors depend on the viewing angle of the fluorescence telescope, α, and the horizontal distance of the light source from the fluorescence detector site. The molecular and aerosol transmission curves look different for two reasons: the horizontal extinction lengths are (slightly) different, $\Lambda^m \sim 18.4$km *versus* $\Lambda^a = 20$km, and the vertical scale heights are *very* different, $h_m \sim 7.5$km *versus* $h_a = 1.2$km (Sokolsky 1996). While any given air shower may be viewed over a wide range of viewing angles the energy measurement is most sensitive in the direction of shower maximum. In this case fluorescence detector viewing angles, $\alpha \approx 10^\circ$, are rather typical.

Implicit in this aerosol model are two assumptions which while true for the molecular atmosphere may not be true for the aerosols. First, that the aerosol vertical variations are much more important than the horizontal variations; *i.e.* we use a 1-dimensional model (not un-typical of the night time atmosphere in large, desert valleys at locations well away from the valley walls). Second, that the vertical profile of the aerosols is the same at all wavelengths in our wavelength interval of interest. Thus we assume that to first order the wavelength dependence is only in the extinction length, $\Lambda^a(\lambda)$.

In the 1-dimensional model described above, two quantities are to be determined: the aerosol horizontal extinction length, $\Lambda^a(\lambda)$ at the altitude of the fluorescence detector sites, and the aerosol optical depth to height, z, above the fluorescence detectors, $\tau^a(z, 355nm)$. These will be measured using dedicated instruments. In all cases the measured quantities include both aerosol and molecular contributions. The aerosol values are obtained by subtracting the molecular (Rayleigh) contributions. This is shown explicitly only for the horizontal extinction length, Sect. 2.1.1.

2.1.1 Horizontal Extinction Length Monitor

The goal of the horizontal extinction length measurement is to determine the combined Rayleigh and Mie horizontal extinction length, $\Lambda(\lambda)$:

$$\frac{1}{\Lambda(\lambda)} = \frac{1}{\Lambda^m(\lambda)} + \frac{1}{\Lambda^a(\lambda)}$$

at several wavelengths, λ, in and near the wavelength acceptance of the fluorescence detectors. The measurement are made at typically one hour time intervals during nights of fluorescence data taking. For the Auger Southern Observatory three identical (but independent) systems monitor three very different light paths across the site. Thus they will provide information on site and instrument related systematic uncertainties in the horizontal extinction length.

The instruments (for each of the three systems) include a stable light source viewed by a stable photometer. Mercury vapor lamps are used as they have strong emission lines into the UV. Transmission measurements are made at wavelengths of 365nm, 405nm, 436nm and 546nm. UV sensitive CCD cameras (Starlight 2000) are used as the photometers. The procedure (Optec 2000) is to measure the intensity at two distances from the source: a *near* measurement a few kilometers from the source and a *far* measurement ~ 50km from the source. The photometer is normally positioned at the *far* location. The *near* measurement is made a few times each year when the photometer is physically moved to a location *near* the light source.

2.1.2 Optical Depth Monitor

The optical depth *versus* height above the fluorescence detectors will be monitored using steerable, backscattered LIDARs. Each backscattered LIDAR consists of a pulsed, 355 nm, laser beam and a receiver telescope. The receiver measures the back-scattered photons as a function of time or equivalently the intensity of the photons *versus* distance to the point the light back-scattered. The observed intensity is given by,

$$I(z,\alpha) = I_0 {\cdot} T_{out} {\cdot} T_{back} {\cdot} \sum_j \frac{1}{\Lambda^j(z)} \frac{1}{\sigma^j} (\frac{d\sigma^j}{d\Omega})_{180^\circ} \cdot \Delta s {\cdot} \Delta\Omega$$

where I_0 is the out-going LIDAR beam intensity, T_{out} and T_{back} are the transmission factors for the (out-going) light beam and for the scattered (back-coming) light respectively, $\Lambda(z)$ are the extinction lengths at height z, $\Delta s = c\Delta t/2$ is the length of the scattering region (set by the LIDAR time bins), $\Delta\Omega$ is the solid angle subtended by the LIDAR mirror, and $\frac{1}{\sigma^j}(\frac{d\sigma^j}{d\Omega})$ are the Rayleigh and Mie *phase functions*. By taking ratios of backscattered LIDAR measurements, $I(z, \alpha)$, from the same altitude, z, but at different angles, α, the phase functions and extinction lengths (which are unknown in the case of aerosol scattering) cancel and the sum of Rayleigh (molecular) and Mie (aerosol) optical depths is obtained.

Backscattered LIDARs will be installed at each of the three fluorescence sites on the periphery of the Auger ground array. Comparison of the three LIDAR results will monitor site and instrument related systematic uncertainties in the optical depth measurements.

2.2 Aerosol Phase Function Monitor

The observed light from an extensive air shower includes both the air fluorescence signal plus some Cherenkov light (mostly in a few degree cone centered on the air shower axis (Baltrusaitis et al., 1987)). Through scattering of the Cherenkov light in the air, some of the Cherenkov light appears as a background in the fluorescence data. To estimate the fraction of Cherenkov light scattered on aerosols we need the aerosol extinction length, at height z above the fluorescence detectors, and the aerosol phase function (normalized aerosol differential scattering cross section) for scattering angles $\geq 10^\circ$ (from the initial light direction).

The observed light from an extensive air shower will also include a contribution of multiple scattered light. This will be true for the air fluorescence signal and for the Cherenkov background light. The size of the correction can be reduced by restricting the time interval (for each photo-tube contributing to the reconstructed shower) and the angular acceptance (transverse to the shower axis) of the data used in shower reconstruction. In making a correction, it is most important to know the Mie phase function at forward scattering angles where Mie dominates Rayleigh scattering.

In the constant composition, 1-dimensional model for aerosols, it is sufficient to measure the aerosol phase function at the altitude of the fluorescence detectors. The measurement can then be made using a near-horizontal, pulsed light beam directed across the field of view of one of the fluorescence sites (Tessier et al., 1999). As each fluorescence detector views $\sim 180^\circ$ in azimuth, even a fixed direction light beam will allow the aerosol phase function to be measured over most of the range of scattering angles. This will be done using a dedicated light source located near at least one of the Auger fluorescence sites. In addition LIDAR beams, from one fluorescence site directed across the field of view (and at near grazing incidence to) adjacent fluorescence sites, provide a good measurement of the small angle aerosol phase function.

2.3 Cross Checks

To monitor and to help minimize systematic uncertainties, all of the atmospheric monitoring measurements are made in at least two independent ways. For example the horizontal extinction length measurement, Sect. 2.1.1, will be compared with horizontal, $\alpha = 0°$, LIDAR measurements. The aerosol optical depth measurement, Sect. 2.1.2, will be compared to measurements from a dedicated star monitor (Raefert 2001). In addition laser *side* scattered light from the LIDAR at one fluorescence site will be observed by the fluorescence detector at a different fluorescence site. A comparison of the predicted *versus* observed signal (as a function of time) provides the essential cross check of the aerosol model and the ingredients of the model: the horizontal extinction length, the vertical profile of aerosols and the aerosol phase function.

2.4 Cloud Detection and Monitoring in Auger

The possible presence of cloud while fluorescence observations are in progress is a cause for concern. The level of cloud cover is a factor in determining the collecting area available to the fluorescence detectors. Unlike smaller cosmic ray experiments, it is quite possible that parts of the atmospheric fiducial volume of the Pierre Auger Observatory will be usable while other parts are not. Additionally, the presence of small, or broken regions of cloud in an otherwise clear sky can lead to uncertainty in the interpretation of shower profiles. The Pierre Auger Project recognized that systematic cloud monitoring in an objective manner was required. This has proved possible using infra-red observations at wavelengths of about 10μm.

Clouds are in a form of thermal equilibrium with their surrounding atmospheric gas. This is at a temperature somewhat below that of the ground and they radiate rather like a black body at wavelengths (of the order of 10μm) appropriate to that temperature. It is then possible to detect clouds by their strong infra-red emission, against a much weaker clear sky background. Such a detector has been described (Clay et al., 1998) based on a Heimann TPS 534 infra-red sensor element.

As noted above, elevation angles of the order of $10°$ will be typical for Auger observations. The atmosphere itself becomes brighter towards the horizon. Experience with the High Resolution Fly's Eye is that a temperature resolution at least as good as 1K is required to efficiently locate cloud at low altitudes. Clear sky emissivity, and hence the brightness close to the horizon, is strongly dependent on atmospheric humidity (Sloan et al., 1955). It is possible to define criteria, including atmospheric humidity information and sky temperatures, which determine the presence of cloud.

In order to make the best use of cloud detectors within the Pierre Auger Observatory, it is both necessary to know that clouds exist and to be able to locate them, preferably in altitude as well as in plan. We are currently examining the use of commercial infra-red imaging cameras to be sited at the three fluorescence sites on the periphery of the Auger ground array. These have temperature resolutions better than 1K. Image processing would determine the existence and angular location of clouds and triangulation between detectors would determine the cloud position in three dimensions. These are likely to be combined with vertical-viewing single pixel radiometers at a subset of the ground array detectors which will help to define cloud front locations at large distances from the cameras.

3 Summary

The major uncertainties in the fluorescence detector measurement of air shower energies were reviewed and the Auger atmospheric monitoring procedures summarized. The Auger monitoring goal is to limit the atmospheric contributions to the shower energy uncertainty to $\sim 10\%$.

Acknowledgements. The atmospheric monitoring procedures and techniques for the Pierre Auger Observatory have build on and profitted from the pioneering work of the High Resolution Fly's Eye (HiRes) collaboration. The Auger procedures have been matured in collaboration with the HiRes and Telescope Array collaborations.

References

Baltrusaitis R. M., et al., 1987 J. Phys. G: Nucl. Phys. **13**, 115
Cassiday, G. L., et al., 1990 Astrophys. J. **356**, 669
Clay R. W., et al., 1998 Pub. Astron. Soc. Aust. **15**, 334
Flowers E. C., McCormick R. A. and Kurfis J. 1969 J. Appl. Meteorology **8**, 955
Kakimoto F., et al., 1996 Nucl. Instrum. Methods **A372**, 527
Martin G. and Matthews J. A. J. 1999 Auger Note: GAP-99-037, http://www-hep.phys.unm.edu/∼johnm/GAP_99_037.pdf
Optec 2000 Model LPV-2 Long Path Visibility Transmissometer, Optec, Inc., 199 Smith Street, Lowell, Michigan, U.S.A.
Raefert, B. 2001 http://concam.net/about.html
Sloan R., Shaw J. H. and Williams D. 1955 J. Opt. Soc. Am. **45** 455
Sokolsky, P. 1996 Proc. of Int. Sym. on Extremely High Energy Cosmic Rays, Ed. M. Nagano, 253
Song C., et al., 1999 astro-ph/9910195
Starlight Xpress HX5 high resolution CCD camera, Starlight Xpress Ltd, Holyport, Berkshire, England SL6 3LA
Tessier, T. et al., 1999 Proc. of 26th International Cosmic Ray Conference, **5**, 408